

Defects and Dopants

Impurity Controlled Dopant Activation: The Role of Hydrogen in the p-type Doping of SiC

B. Aradi[1], P. Deak[1], E. Janzén[2], R. P. Devaty[3], W. J. Choyke[3]
[1]Budapest University of Technology and Economy Hungary; [2]Linköping University, Sweden; [3]University of Pittsburgh, USA

Incorporation of Hydrogen (1H and 2H) in 4H-SiC during Epitaxial Growth

M. K. Linnarsson[1], U. Forsberg[2], M. S. Janson[1], E. Janzén[2], B. G. Svensson[1,3]
[1]Royal Institute of Technology, Sweden; [2]Linköping University, Sweden; [3]University of Oslo, Norway

Physical Mechanism for the Anomalous Behavior of n-type Dopants in SiC

R. K. Malhan[1], J. Kozima[1], T. Yamamoto[1], A. Fukumoto[2]
[1]DENSO Corporation, Japan; [2]Toyota Central R&D Labs., Inc., Japan

Damage Evolution and Recovery in Al-Irradiated 4H-SiC

Y. Zhang[1], W. J. Weber[2], W. Jiang[2], A. Hallén[3], G. Possnert[1]
[1]Ångström Laboratory, Sweden; [2]Pacific Northwest National Laboratory, USA; [3]Royal Institute of Technology, Sweden

Comparison between Chemical and Electrical Profiles in Al or N Implanted and Annealed 6H-SiC

R. Nipoti[1], A. Carnera[2], V. Raineri[3]
[1]Istituto LAMEL, Italy; [2]Dipartimento di Fisica and INFN, Italy; [3]Istituto IMETEM, Italy

Polytype-Dependence of Transition Metal Related Deep Levels in 4H, 6H, and 15R-SiC

J. Grillenberger[1], N. Achtziger[2], G. Pasold[1], W. Witthuhn[1]
[1]Universität Jena, Germany; [2]Fraunhofer Institut IIS-A, Germany

Electronic Localization Around Stacking Faults in Silicon Carbide

H. Iwata[1], U. Lindefelt[2], S. Öberg[3]
[1]Linköping University, Sweden; [2]ABB Corporate Research, Sweden; [3]Luleå Technical University, Sweden

Impurity Controlled Dopant Activation : The Role of Hydrogen in the p-type Doping of SiC.

B. Aradi¹, P. Deák¹, E. Janzén², R. P. Devaty³, and W. J. Choyke³

¹Department of Atomic Physics, Budapest University of Technology and Economics, Budafoki út 8, Budapest, H-1111, Hungary

phone: [36]-(1)-463-4207, fax: [36]-(1)-463-4357, e-mail: p.deak@eik.bme.hu

²Department of Physics and Measurement Technology, Linköping University, Linköping, S-58183, Sweden

³Department of Physics and Astronomy, University of Pittsburgh, Pittsburgh, PA 15260, USA

Hydrogen is a natural contaminant of the SiC growth processes and may occur in large quantities in as grown epilayers. Its presence might affect doping efficiency by influencing the site competition process or by passivating or compensating the dopants. Passivation by complex formation with hydrogen has been proven both for Al and B [1], however, the experimentally observed reactivation energies seem to differ by about ~1 eV [2]. Furthermore, hydrogen incorporation proportional to that of boron was observed in B-doped as grown CVD samples [3,4] while the amount of hydrogen was found to be two orders of magnitude less than the aluminum concentration in case of Al-doping [5].

Extensive calculations regarding geometry and formation energy of *p*-type substitutional dopants (B, Al) and their complexes with hydrogen have been carried out. The local density approximation of the density functional theory was used with plane wave basis and norm-conserving pseudopotentials. Our results indicate that hydrogen plays a key role in the in-growth doping of epilayers with boron. In the absence of hydrogen, boron prefers the carbon site. If hydrogen is present, as in typical CVD conditions, boron is incorporated together with hydrogen (in equal amounts) and the B+H complex favors the silicon site. Annealing around 500 °C may remove hydrogen leaving the Si site substitutional boron behind. Since boron at different sites gives rise to different electrical activities, the effect of hydrogen influences its activation as a shallow acceptor.

In contrast to boron, aluminum is always incorporated as isolated substitutional at the silicon site, independent of the presence of hydrogen. The calculated amount of incorporated hydrogen in that case is in good agreement with experimental findings for aluminum doped samples. Dissociation of the stable dopant plus hydrogen complexes for boron and aluminum has also been investigated. Our calculations yields a dissociation energy difference of ~0.9 eV between the stable B+H and Al+H complexes, in good agreement with experiment. Characteristic local vibration modes of the complexes are predicted.

[1] M. S. Janson, A. Hallén, M. K. Linnarsson, N. Nordell, S. Karlsson, and B. G. Svensson, *Mater. Sci. Forum* **353-356**, 427 (2001).

[2] M. S. Janson, M. K. Linnarsson, A. Hallén, and B. G. Svensson, to be published

[3] D. J. Larkin, *phys. stat. sol. (b)* **202**, 305 (1997).

[4] A. Henry, B. Magnusson, M. K. Linnarsson, A. Ellison, M. Syväjärvi, R. Yakimova, and E. Janzén, *Mater. Sci. Forum* **353-356**, 373 (2001).

[5] M. K. Linnarsson, M. S. Janson, and B. G. Svensson, to be published.

Incorporation of Hydrogen (^1H and ^2H) in 4H-SiC during Epitaxial Growth

M.K. Linnarsson^{1*}, U. Forsberg², M.S. Janson¹, E. Janzén² and B.G. Svensson^{1,3}

¹ Royal Institute of Technology, Solid State Electronics, P.O. Box E229, SE-164 40 Kista-Stockholm, Sweden

² Linköping University, Department of Physics and Measurement Technology, SE-581 83 Linköping, Sweden

³ University of Oslo, Department of Physics, Physical Electronics, P.B. 1048 Blindern, N-0316 Oslo, Norway

* Phone: +46-8-752 1412, Fax: +46-8-752 7782, email: marga@ele.kth.se

Hydrogen in semiconductors is known to be trapped by donors and acceptors as well as “dangling bonds” in vacancies, dislocations and grain boundaries [1]. The presence of hydrogen can drastically change the electronic properties and strongly influence device performance. In SiC technology hydrogen is extensively used and there are many opportunities to introduce hydrogen into SiC structures [2]. Redistribution may occur during subsequent annealing steps. In p-type SiC hydrogen will form complexes with boron and aluminum acceptors [3,4]. Unfortunately, possible hydrogen trapping centers in n-type are not well documented. Trapping centers are actually necessary to detect the migrating hydrogen with secondary ion mass spectrometry (SIMS) since free hydrogen diffuses at concentration levels well below the detection limit.

In this work we have studied the incorporation of deuterium (^2H) and normal hydrogen (^1H) from the carrier gas during epitaxial growth. SIMS has been utilized to obtain the depth distribution of hydrogen. There are two reasons for the use of ^2H in combination with ^1H . First ^2H relative to ^1H increase the SIMS-sensitivity by three orders of magnitude and second, sequential use of ^1H and ^2H gives information about when hydrogen is retained in SiC. 4H-SiC epitaxial structures with alternating aluminum and nitrogen doped layers separated by undoped material have been grown at 1600°C (see Fig. 1). A mixture of 77% ^2H and 23% ^1H (in total 13 l/min) were used as carrier gas during the growth of the first four doped layers while only ^1H (13 l/min) was employed for the growth of the remaining structures and cool down procedure. The same type of structure has also been grown starting with pure ^1H followed by a deuterium mixture as carrier gas. Both n and p-type substrates have been used.

Fig. 1 shows that ^1H get trapped in a heavily Al doped layer. Deuterium is also detected in this layer at a concentration close to natural abundance (0.015%). In this case the second part of the growth and the cooling down procedure has been performed in a $^1\text{H}_2$ ambient. Besides from the layer of the highest Al content the ^2H concentration is below detection limit, $1 \times 10^{14} \text{ cm}^{-3}$. When the sequence of used carrier gases is changed i.e. the deuterium mixture is used in second part of the epitaxial growth no ^1H is recorded in the sample above the detection limit ($1 \times 10^{17} \text{ cm}^{-3}$). ^2H is found in layers with Al concentrations above $5 \times 10^{17} \text{ cm}^{-3}$ while ^2H is below the detection limit in the N doped layers. However, the ^2H concentration in both n-type and p-type substrates are $1 \times 10^{15} \text{ cm}^{-3}$.

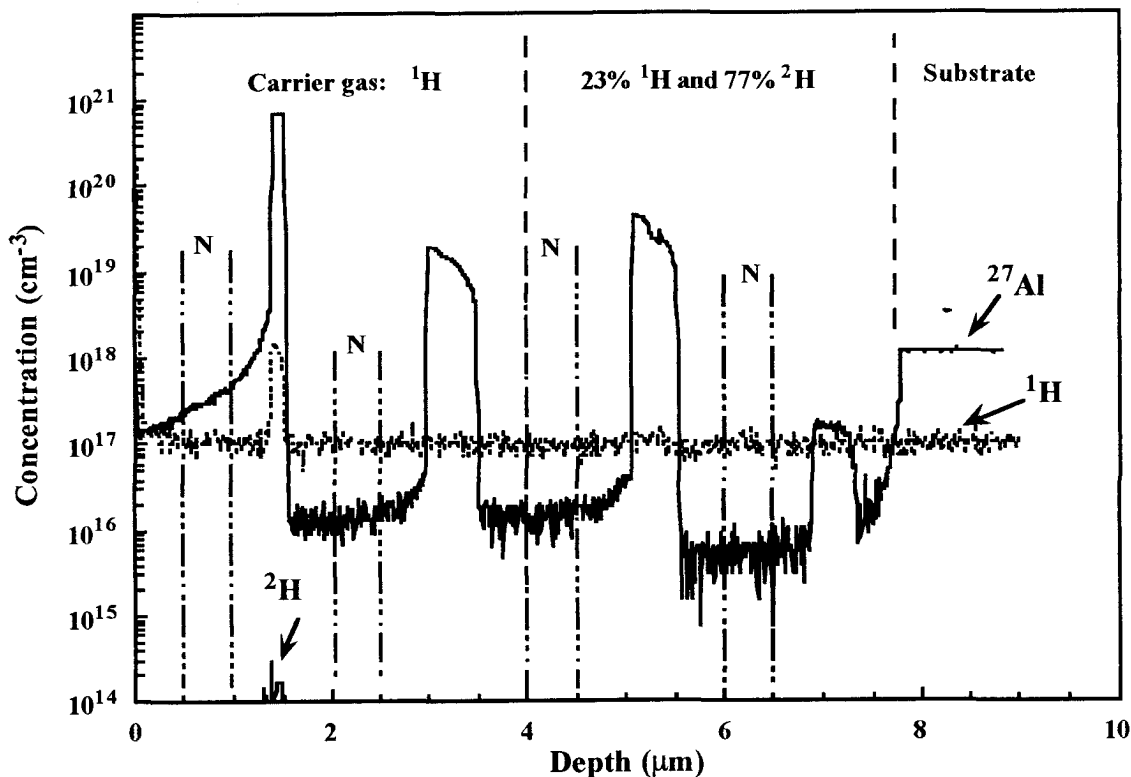


Fig.1. SIMS measurement of depth distribution of ¹H and ²H in an Al and N doped epitaxial grown 4H-SiC structure. A mixture of ²H and ¹H has been used in the first part of the growth and pure ¹H has been employed in the second part and during cool down.

Our results show a very high mobility for hydrogen in SiC at the growth temperature, 1600°C. Only the carrier gas (¹H or ²H) used at the later part of the epitaxial growth will be incorporated in SiC. Hydrogen may be incorporated in both p- and n-type SiC if suitable traps are available. Comparing the ²H incorporation in the epitaxial structures and n-substrate eliminates N as a probable trapping center for hydrogen. The difference between the Al to ²H ratio in the epitaxial material and the p-type substrate indicates that Al may not be the main hydrogen trap in the substrate. Furthermore, if the hydrogen concentration is constant through the whole substrate (thickness ~0.4 mm) it will be a large hydrogen source, which may redistribute in subsequent annealing steps.

- [1] J.I. Pankov and N.M. Johnson, *Hydrogen in semiconductors* (Academic Press, New York, 1991).
- [2] D.J. Larkin, S.G. Sridhara, R.P. Devaty et al., *J. Electr. Mat.* **24**, 289 (1995).
- [3] M.K. Linnarsson, M. Janson, S. Karlsson et al., *Mat. Sci. and Eng.* **B61-62**, 275 (1999).
- [4] M.S. Janson, A. Hallén, M.K. Linnarsson et al., *Mat. Sci. Forum* **353**, 427 (2001).

Physical mechanism for the anomalous behavior of n-type dopants in SiC

Rajesh Kumar Malhan, Jun Kozima, Tsuyoshi Yamamoto, and Atsuo Fukumoto*

Research Laboratories, DENSO CORPORATION, Komenoki-cho, Nisshin, Aichi 470-0111, Japan
Tel: +81-5617-5-1016; Fax: +81-5617-5-1193; E-mail: kumar@rlab.denso.co.jp

*Toyota Central Research and Development laboratories, Inc., Nagakute, Aichi 480-1192, Japan

The selective doping of SiC by ion-implantation is a key process for fabricating the planar devices. A donor (N, P, As) and an acceptor atoms (Al, B, Ga) are required for the tailored n- and p-type doping profiles. Recent reports on n-type SiC doping indicate that P is a potential candidate for power device applications which require low source/drain contact resistance. Capano et al.[1] reported that P is the better choice for the high doses due to higher electron mobility, however, N is preferred for the moderate doping levels. Khan et al.[2] reported about four times lower dielectric strength of thermal oxide grown over a P implanted region than a non-implanted region and about two times lower than the N implanted region under the identical conditions. However, the average ionization energies (h- and k-lattice sites) of the P donor is relatively higher than that of the N donor in 4H-SiC. A physical explanation for the P and N anomalous behavior is needed, although this is usually correlated with the dopant lattice site difference and/or the high implantation-induced lattice damage by P due to heavier atomic mass than N atom. In this work, we carefully investigated the electrical activation of P, N, P+N (identical profiles) and P/N (sequential profiles) implanted 4H-SiC and also considering the first principle calculations for a possible physical mechanism. The P and N implantations were performed at elevated temperatures to minimize implantation-induced lattice damage[3] and subsequently annealed at temperatures in the range of 1200~1700°C for 30 min. in Ar gas ambient. The electrical activation investigations indicate an order of magnitude lower sheet resistance for P implanted samples compare to the N implanted one at higher annealing temperatures as shown in Fig.1. We also observed that at lower annealing temperature around 1200°C, the sheet resistance for P or N implanted 4H-SiC is relatively higher than that for the P+N or P/N implanted samples (Sheet resistance > 1kΩ/sq.). However, at higher activation annealing temperature, there was no remarkable difference in the sheet resistance of the P single or co-implanted 4H-SiC. Sheet resistance of N implanted samples were higher in the entire annealing temperature range. These results indicate that it may be possible to reduce the thermal budget for device processing simply by considering the P and N co-implantation as well as the pn leakage currents by trimming and/or tailoring the implantation profiles.

For a possible physical explanation of the experimental results, we calculated the electronic structure of N and P donor substitutional models. The calculations are based on the local density functional (LDF) approximation and norm-conserving pseudopotential method[4]. A 64-atom cubic super cell structure was considered to study the dopant interactions under the high doses of implanted species. Considering that N has atomic covalent radius and electro-negativity values more close to the C-atom compare to Si-atom. The probability of N to occupy the C-lattice site is very high, compare to Si-lattice site. Earlier, we reported that the N dopant on the C-lattice site (N_C) acts as a shallow donor ($\Delta E=180\text{meV}$). Similarly, the probability of P to occupy the Si-lattice site (P_{Si}) is very high in SiC, therefore, acts as a shallow donor ($\Delta E=680\text{meV}$). The co-implantation of P and N can extend the maximum obtainable activation by occupying both C- and Si-lattice site, respectively. The calculated square wave function of the half-occupied highest state of considered models, which is equivalent to the donor densities is shown in Fig.2. The donor density of $Si_{32}C_{30}N_2$ models is widely spread over the crystal. The density is high at the anti-bonding sites around Si atoms. The calculated eigen values of substitutional models are summarized in Table-1. The absolute values of the eigen values are not realistic because of the small size of the model ($Si_{32}C_{32}$) considered for the present calculations. The presence of two N atoms in very close vicinity results in the eigen value shift (ΔE_{shift}) of about 140meV. Similarly, the donor density of $Si_{30}C_{32}P_2$ model is also well spread over the crystal and ΔE_{shift} of about 50meV was observed. The difference of electro-negativity between Si and P is less than that of C and N. In $Si_{31}C_{31}PN$ model, as the donor density around N and P have different symmetries, therefore, the overlap between these wave functions is small compare to $Si_{32}C_{30}N_2$ and $Si_{30}C_{32}P_2$ models. The shallow levels will not be disturbed in case of high doses of implanted species.

The ΔE_{shift} of about 20meV and 40meV was observed for N and P, respectively in the $\text{Si}_{31}\text{C}_{31}\text{PN}$ model. These calculations confirm that the co-implantation of P and N can extend the maximum obtainable activation for the n-type SiC doping by implantation. In addition, the excess Si interstitials generated during the P implantation process leads to the formation of C vacancies (V_C) that works as a shallow donor level ($\Delta E=10\text{meV}$). The formation of V_C , thus the shallow donor level can explain the observed low sheet resistance for P doped SiC, compare to the N doped one. Also, the possible cause for the lower activation for N doped SiC is either due to the dopant interactions that results in the large ΔE_{shift} or due to presence of excess C atoms in the SiC lattice. The excess C atoms either occupies Si-lattice site (C_{Si}) or interstitial position to form complex defects with substitutional N, which produces a localized electronic state [3,5]. The experimental data also supports the hypothesis that the dopants that occupies the C-lattice site, leads to lower activations as compare to the one that occupies the Si-lattice site.

References

[1]. M. A. Capano, *MRS Fall Meeting*, Boston, 2000.
 [2]. I. A. Khan, B. Um, M. Matin, M. A. Capano, and J. A. Cooper Jr., *MRS Fall Meeting*, Boston, 2000.
 [3]. T. Miyajima, N. Tokura, A. Fukumoto, H. Hayashi, and K. Hara, *Jpn. J. Appl. Phys.*, 35(1996)1231.
 [4]. A. Fukumoto, *Phys. Rev. B*, 53 (1996) 4458.
 [5]. R.K. Malhan, *Int. Workshop on Ultra-Low Loss Power Devices*, Nara, 2000.

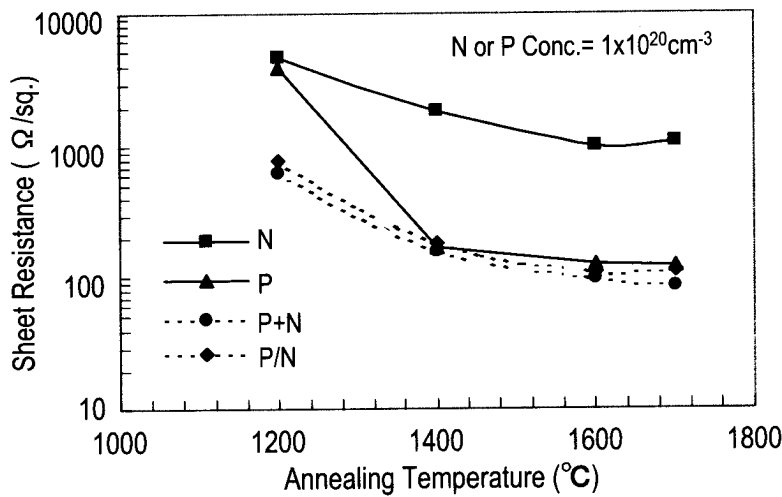


Fig.1 Dependence of sheet resistance of N, P, P+N (identical profiles), and P/N (sequential profiles) implanted 4H-SiC on the activation annealing temperature.

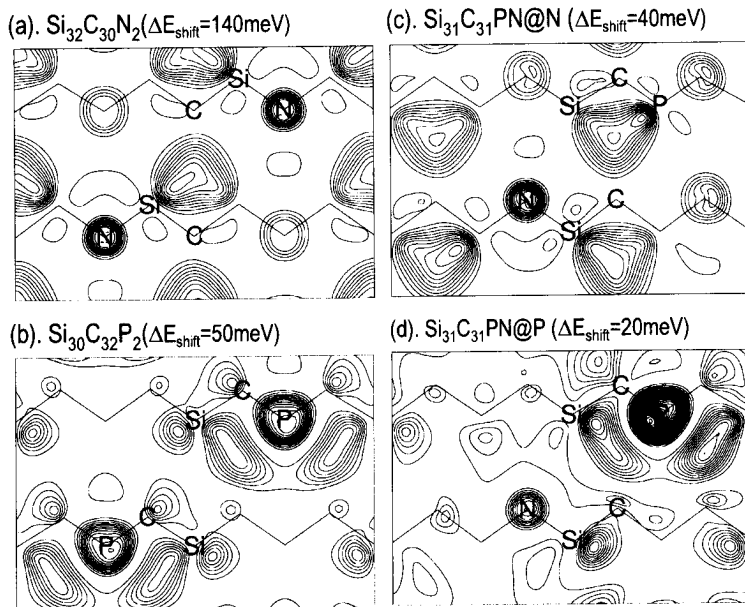


Table-1: Eigen values of impurity states*

	$\text{Si}_{32}\text{C}_{31}\text{N}$	$\text{Si}_{31}\text{C}_{32}\text{P}$
N-atom (meV)	180	
P-atom (meV)		680

(*64atom super cell cubic model)

Fig.2 Square wave function of the impurity state around the (a) N atom in the $\text{Si}_{32}\text{C}_{30}\text{N}_2$ model, (b) P atom in the $\text{Si}_{30}\text{C}_{32}\text{P}_2$ model, (c) N atom in the $\text{Si}_{31}\text{C}_{31}\text{PN}$ model, and (d) P atom in the $\text{Si}_{31}\text{C}_{31}\text{PN}$ model. The contour spacing is 0.0004au (e/Bohr^3).

Damage evolution and recovery in Al-implanted 4H-SiC

Y. Zhang¹, W. J. Weber², W. Jiang², A. Hallén³, G. Possnert¹

¹ Division of Ion Physics, Ångström Laboratory, Box 534, SE-751 21, Uppsala, Sweden

² Pacific Northwest National Laboratory, PO Box 999, Richland, WA 99352, USA

³ Department of Microelectronics and IT, Royal Institute of Technology, Electrum 229, SE-164 40 Stockholm, Sweden

Epitaxial growth 4H-SiC layers have been implanted with 1.1 MeV Al₂²⁺ molecular ions at a tilt angle of 60° relative to the surface normal to fluences ranging from 1.5×10¹³ to 8.00×10¹⁴ Al cm⁻² at 150 K. Isochronal annealing for 20 minutes was performed from 200 up to 870 K. Damage evolution and recovery on the Si and C sublattices have been studied simultaneously using in situ Rutherford backscattering spectroscopy and nuclear reaction analysis along the <0001> channeling direction (RBS/C and NRA/C), as well as at an off-channel direction (RBS/R), with 0.94 MeV D⁺ and 2.0 MeV He⁺ at a scattering angle of 150° relative to the incoming beam. The in situ RBS/C and NRA/C spectra from samples implanted with various ion fluences are shown in Fig. 1, along with random and virgin spectra. The results indicate the increase in disorder on both the Si and C sublattices with increasing ion fluences. Once the random level is reached, the width of the damage peak also increases with further irradiation.

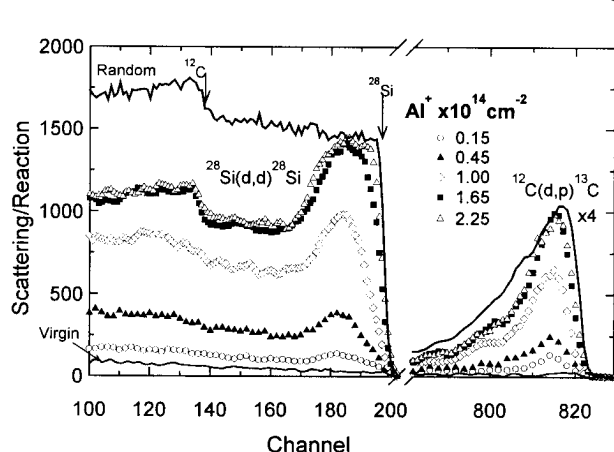


Fig. 1. RBS/C and NRA/C spectra for 4H-SiC irradiated with 1.1 MeV Al₂²⁺ molecular ions to different ion fluences at 150 K measured with 0.94 MeV D⁺.

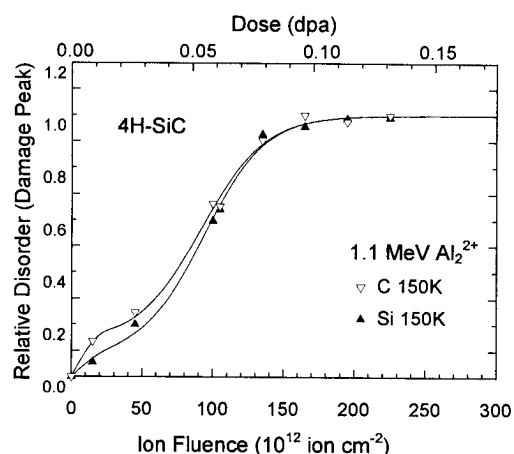


Fig. 2. Relative disorder as a function of ion fluence at the damage peak for 1.1 MeV Al₂²⁺ implanted 4H-SiC at 150 K.

The depth profiles of relative disorder on the Si and C sublattices were determined from the RBS/C and NRA/C spectra using the ratio of aligned spectra to random spectra and correcting for the background dechanneling fraction. The relative disorder on the Si and C sublattices at the damage peak is shown in Fig. 2 as a function of the ion fluence and local dose (dpa). The results indicate a departure at this irradiation temperature from the sigmoidal dependence that is normally observed at higher temperatures. The higher rate of C disordering at low ion fluences is consistent with the low threshold displacement energies for C atoms.

Isochronal annealing was carried out sequentially at temperatures from 200 up to 870 K. The relative residual disorder at the damage peak for both the Si and C sublattices after annealing

is shown in Fig. 3 for 0.45 and 1.65×10^{14} Al cm^{-2} samples. Three distinct recovery stages are present in Fig. 3. At low ion fluences (4.5×10^{13} Al cm^{-2}), where the damage states are far below the fully amorphous state, two distinct recovery stages are observed on both the Si and C sublattices. The first recovery stage (I) occurs between 250 and 420 K, and the second recovery stage (II) occurs between 470 and 570 K. At intermediate ion fluences (1.65×10^{14} Al cm^{-2}), where the relative disorder is just below the fully amorphous state, the first stage is largely absent while second stage is still present; however, a third recovery stage (III) is observed between 600 and 700 K. At high irradiation fluences, where a buried amorphous layer is produced ($>1.95 \times 10^{14}$ Al cm^{-2}), the onset of a fourth recovery stage (not shown) is observed above 800 K. A more detailed description of the recovery processes over the range of ion fluences from 1.5×10^{13} to 2.25×10^{14} Al cm^{-2} will be presented, and the recovery stages will be more apparent, since the amount of specific recovery in each stage depends on the initial damage state prior to annealing.

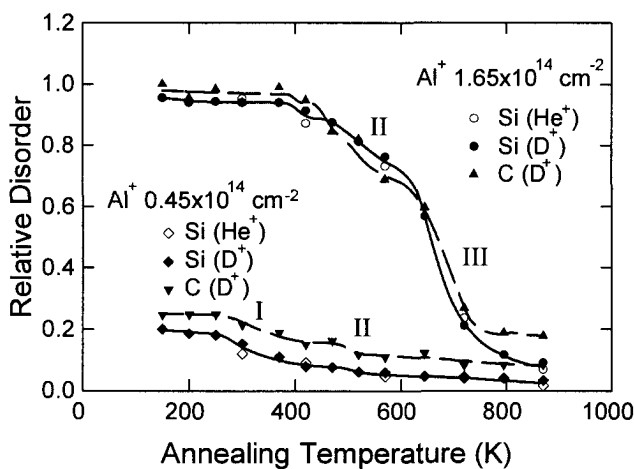


Fig. 3. Isochronal recovery of relative disorder for both Si and C sublattices at the damage peak

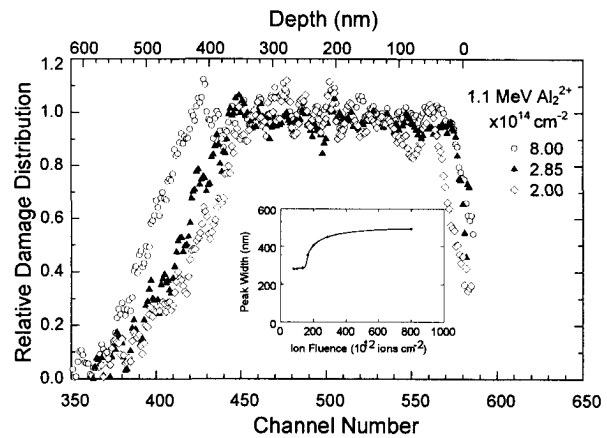


Fig. 4 Profiles of the relative damage distribution along $\langle 0001 \rangle$ at 300 K in 4H SiC irradiated with 1.1 MeV Al^{2+} . The inner plot is the width of as-implanted damage peak as a function of ion fluence.

Fig. 4 shows the profiles of the relative damage distribution along $\langle 0001 \rangle$ at 300 K for the Si sublattice as a function of channel number and depth in 4H-SiC implanted with high fluences. The inner plot indicates the width (FWHM) of the damage peak or the amorphous layer as a function of ion fluence. The width keeps constant at lower ion fluences, and increases significantly when close to the critical amorphization dose (Fig. 2) of 0.11 dpa or 1.90×10^{14} Al cm^{-2} . The thickness of the amorphous layer increases at a reduced rate with further irradiation. Different thicknesses of the amorphous layers and damage levels just below the surface were produced by irradiation of 2.00, 2.85 and 8.00×10^{14} cm^{-2} as shown in Fig. 4. After isochronal annealing, different crystal recovery can be observed. For the lower fluence implanted samples, the crystal recovery occurs from both the front and rear amorphous/crystal interfaces. For the 8.00×10^{14} cm^{-2} irradiated samples, the crystal re-growth starts only from the rear interface. The nonlinear temperature dependence of the recrystallization is attributed to distinct recovery processes.

COMPARISON BETWEEN CHEMICAL AND ELECTRICAL PROFILES IN AL⁺ OR N⁺ IMPLANTED AND ANNEALED 6H-SiC.

R. Nipoti^a, A. Carnera^b and V. Raineri^c

^aCNR-IMM Istituto LAMEL, via Gobetti 101, 40129 Bologna, Italy,
 tel. +39 051 6399147
 fax +39 051 6399216
 e-mail nipoti@lamel.bo.cnr.it

^bDipartimento di Fisica and INFM, Università degli Studi di Padova, via Marzolo 8,
 35131 Padova, Italy

^cCNR-IMM Istituto IMETEM, Stradale Primosole 50, 95121 Catania, Italy

This work compares the measurements of chemical and electrical profiles in ion implanted and annealed 6H-SiC samples. Secondary Ion Mass Spectrometry (SIMS) and Scanning Capacitance Microscopy (SCM) were used to measure the first and the latter profiles, respectively.

6H-SiC <0001> bulk wafers with a carrier concentration in the decades 10¹⁷-10¹⁸ cm⁻³ were used. Al⁺ and N⁺ ions were implanted in n- and p-type wafers, respectively, at various energies and fluence values so to produce an almost box shape profile about 1 μm thick at the sample surface with a plateau concentration in the decade 10¹⁹ cm⁻³. The implantation and annealing temperatures were 300°C and 1700°C, respectively. The annealing was done in a RF furnace in Ar ambient and was 30 min long.

The structural analysis of the recovered layers showed the presence of a weak density of secondary defects which perturbed the crystal lattice preferentially along the planar (11-20) and (10-10) directions than along the axial <0001> one, as described in [1].

Figs 1 and 2 show the comparison between SIMS and SCM profiles for both the p- and the n-type implanted species. The profile shapes qualitatively agree except for the junction depth value. Taking into account that both the diagnostic techniques claim a depth resolution equal to 10-20 nm, such a difference remains a puzzle to solve. This remark can be done: the relative position of the chemical to the electrical junction depth is the same with respect to the n- and p-type sides of any sample.

Hall measurements are in progress to convert the SCM capacitance profiles in carrier density profiles. That is possible because, in spite of the high doping level of the substrates, p/n junction were formed.

[1] R. Nipoti, A. Carnera and G. Mattei, MRS Proceedings Vol. 690 (2001) paper H5.28, in press

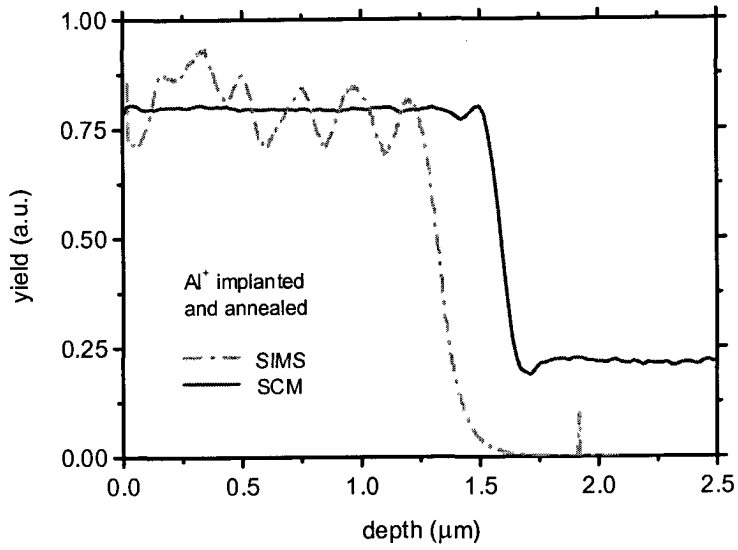


Fig. 1. Comparison between the SIMS and the SCM profiles for the sample Al⁺ implanted.

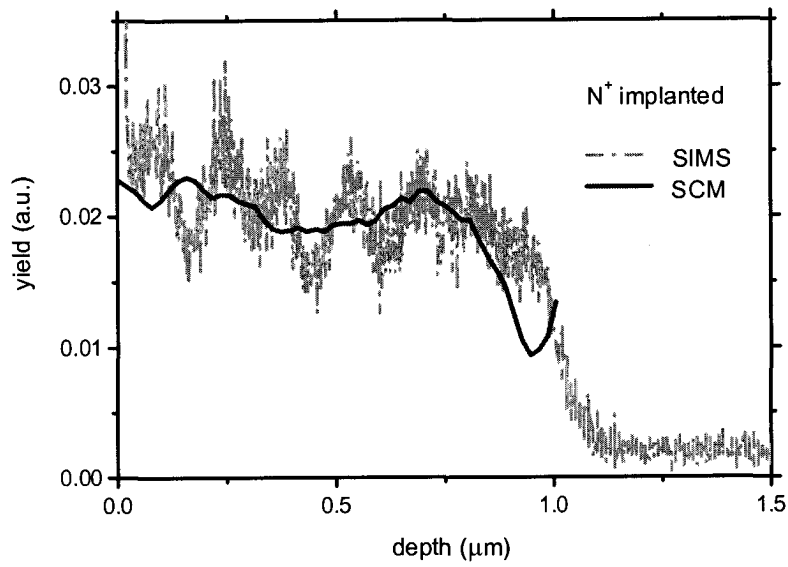


Fig. 2. Comparison between the SIMS and the SCM profiles for the sample N⁺ implanted.

POLYTYPE-DEPENDENCE OF TRANSITION METAL-RELATED DEEP LEVELS IN 4H-, 6H AND 15R-SiC

J. Grillenberger¹, N. Achtziger², G. Pasold¹, W. Witthuhn¹

¹Institut für Festkörperphysik, Universität Jena, Max Wien Platz 1, 07743 Jena, Germany

²Fraunhofer Institut für Integrierte Schaltungen IIS-A, Am Weichselgarten 3, D-91058 Erlangen, Germany

Besides the known deep level data of Ti, Cr, V in the polytypes 4H- and 6H-SiC [1-4], we present additional results and thus provide an extensive data set about deep levels of transition metals in silicon carbide (SiC). The data were obtained by means of Radiotracer Deep Level Transient Spectroscopy (DLTS) involving radioactive isotopes of the elements of interest. Observing characteristic concentration changes of deep levels during the radioactive decay by means of repeated DLTS-measurements we could definitely identify deep levels of Ti, Cr, V, Ta, and W in the band gap of the three SiC-polytypes investigated (see Fig.1).

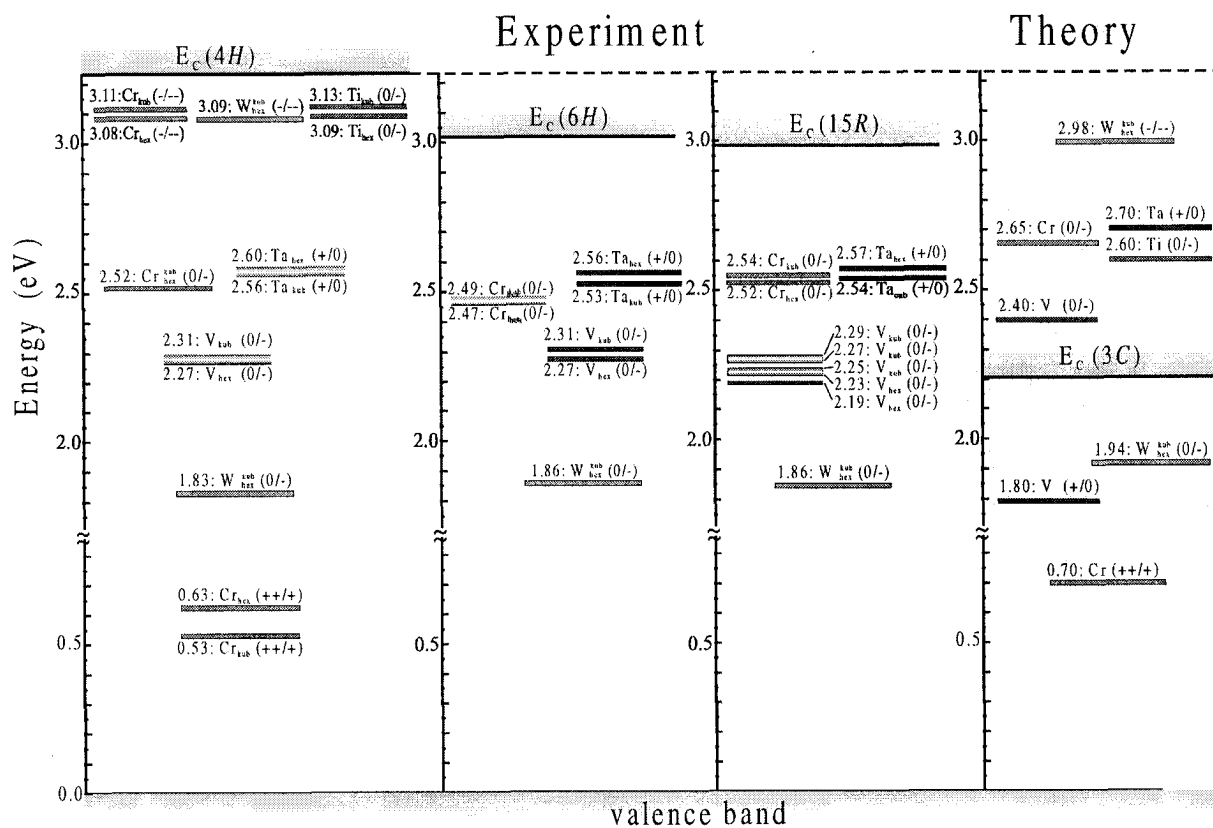


Fig.1: Energy scheme of the SiC polytypes 3C, 4H, 6H, and 15R. It is based on the assumption, that the valence bands of the SiC polytypes are energetically aligned [6]. The trap positions in the band gap of the polytypes are given by their energetical distance to the valence band. The values for 3C-SiC are theoretical predictions [8].

The level energies of each element in 4H-, 6H-, and 15R-SiC are compared and the conduction band offsets between the polytypes are derived according the Langer-Heinrich rule [5]. Obviously the valence bands of all polytypes are energetically aligned. This fact is also confirmed by other experimental [6] as well as theoretical studies [7]. Considering this information and the rule of Langer and Heinrich we present a comparison between the experimental data and theoretically predicted values [8] for the trap energies of transition metals in SiC. If we also include conduction band resonances, the theoretical and experimental data concerning level energies are in good agreement.

Some transition metals (Cr, V, Ta, Ti) exhibit a level splitting of there corresponding deep state. This splitting is due to the occupation of inequivalent lattice sites in SiC and varies in magnitude depending on the investigated polytype and/or element. Though, the level splitting does not affect the application of rule of Langer and Heinrich in SiC. To energetically align the trap positions it is sufficient to calculate a mean activation energy in each polytype.

For all polytypes investigated (4H-, 6H-, 15R-SiC), the splitting of the V levels is larger than for other elements and increases from 4H-, over 6H- to 15R-SiC. The same tendency is observed for Cr where a splitting is resolved by DLTS in the polytype 15R only.

- [1] V.A. Il'in, V.A. Ballandovich, Defect and Diffusion Forum, 103-105 (1992) 633.
- [2] N. Achtziger, J. Grillenberger, W. Witthuhn, Appl. Phys. A 65 (1997) 329.
- [3] N. Achtziger, W. Witthuhn, Appl. Phys. Lett. 71 (1997) 110.
- [4] T. Dalibor, G. Pensl, H. Matsunami, T. Kimoto, W.J. Choyke, A. Schöner, N. Nordell, phys. stat. sol. (a)162 (1997) 199.
- [5] J.M.Langer and H.Heinrich, Phys.Rev.Lett. 55 (1997) 1414.
- [6] V.V.Afanas'ev, M.Bassler, G.Pensl, M.J.Schulz, and E.Stein von Kamienski, J.Appl.Phys. 79 (1996) 3108.
- [7] P.Käckell, B.Wenzien, and F.Bechstedt, Phys.Rev.B 50 (1994) 10761.
- [8] H. Overhof, University of Paderborn, private communication

corresponding author: Tel. +49 (0)3641-947337, Fax: +49 (0)3641-947302, e-mail: jojo@pinet.uni-jena.de

Electronic localization around stacking faults in silicon carbide

Hisaomi Iwata^{a)}, Ulf Lindefelt^{a,b)}, and Sven Öberg^{c)}

^{a)}Department of Physics and Measurement Technology, Linköping University, SE-58183 Linköping, Sweden

^{b)}ABB Corporate Research, SE-72178 Västerås, Sweden

Phone:+46 21 32 3177, Fax:+46 21 32 3212, Email:Ulf.Lindefelt@secrec.abb.se

^{c)}Department of Mathematics, Luleå Technical University, SE-97187 Luleå, Sweden

In order to fully develop SiC based technology, there are still material problems that need to be understood. One such problem is the occurrence of stacking faults (SF). In general, the SF energy of SiC is believed to be very small (around 3mJ/m^2 and 15mJ/m^2 for 6H- and 4H-SiC, respectively) compared to other semiconductors such as Si (55mJ/m^2), diamond (280mJ/m^2), or GaAs (45mJ/m^2) [1-3]. Because of the small SF energy it is relatively easy to develop extended SF regions in SiC crystals, which, if electrically active, can seriously affect device performance.

We report on a first-principles study of all the structurally different SFs that can be introduced by glide along the (0001) basal plane in 3C-, 4H-, and 6H-SiC (see Fig.1), based on the local-density approximation within the density-functional theory. Our band structure calculations using supercells containing 96 atoms have revealed that both types of SF in 4H-SiC, and two of the three different SFs in 6H-SiC (type I and II), give rise to quasi-2D energy band states in the band gap at around 0.2 eV below the lowest conduction band (see Fig.2), thus being electrically active in n-type material. Although SFs, unlike point defects and surfaces, are not associated with broken or chemically perturbed bonds, we find a strong localization, within roughly 10-15 Å, perpendicular to the SF plane, of the wave functions of the SF gap states in both 4H- and 6H-SiC (see Fig.3). In 3C- and type III SF in 6H-SiC, the states in the immediate vicinity of the valence band maximum show some degree of localization, as do also the states in the vicinity of the lowest conduction band for type III SF in 6H-SiC. These states are less localized, however, than the gap states for the SF of type I and II in 4H- and 6H-SiC. We find that this quantum-well-like feature of certain SFs in SiC can be understood in terms of the large conduction band offsets between the cubic and hexagonal polytypes [4].

[1] M. H. Hong, A. V. Samant, and P. Pirouz, *Phil. Mag. A*, **80**, 919 (2000).

[2] K. Maeda, K. Suzuki, S. Fujita, M. Ichihara, and S. Hyodo, *Phil. Mag. A*, **57**, 573 (1988).

[3] P. Käckell, J. Furthmüller, and F. Bechstedt, *Phys. Rev. B*, **58**, 1326 (1998).

[4] H. Iwata, U. Lindefelt, and Sven Öberg, submitted to *Phys. Rev. Lett.*

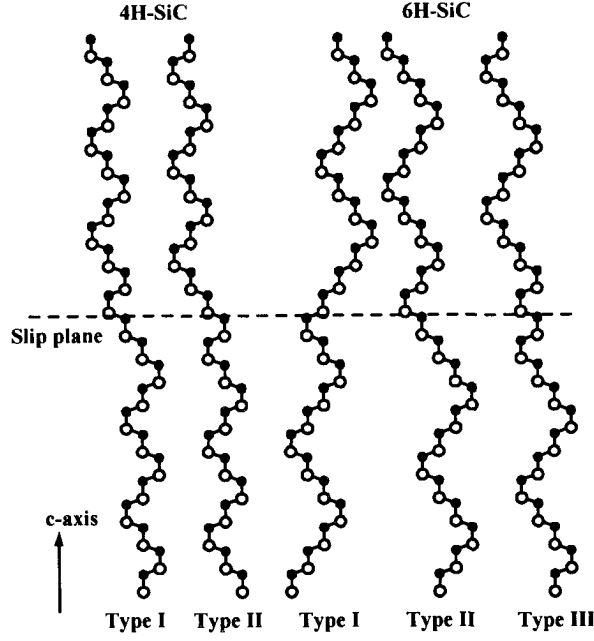


Fig. 1. Geometrically distinguishable SFs in 4H- and 6H-SiC

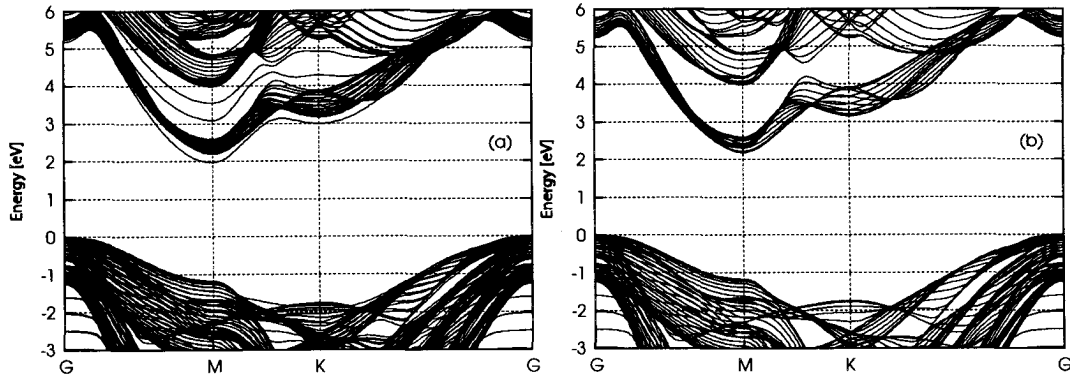


Fig. 2. Band structures of 4H-SiC (a) with and (b) without SF of type I.

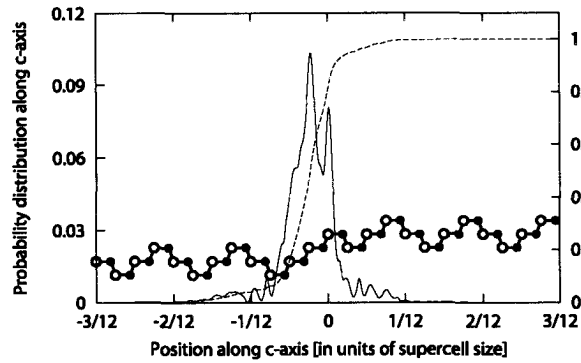


Fig. 3. Squared wave function distribution along the c -axis, $f(z) = \iint |\psi(x, y, z)|^2 dx dy$, where the integration for each value of z along the c -axis is performed in the basal plane within the supercell for the wave function at the M-point for the split-off conduction band in 4H-SiC with SF type I. The normalization integral, $I(z) = \int^z f(z') dz'$, is also shown (right y-axis), together with the corresponding stacking sequence.